Gigantic Kerr rotation induced by a *d-d* transition resonance in $M\mathrm{Cr}_2\mathrm{S}_4$ (M=Mn,Fe)

K. Ohgushi,[1] T. Ogasawara,[2] Y. Okimoto,[2] S. Miyasaka,[1] and Y. Tokura[1,2,3]
[1]*Department of Applied Physics, University of Tokyo, Tokyo 113-8656, Japan*
[2]*Correlated Electron Research Center (CERC), National Institute of Advanced Industrial Science and Technology (AIST), Tsukuba 305-8562, Japan*
[3]*Spin Superstructure Project (SSS), ERATO, Japan Science and Technology Corporation (JST), Tsukuba 305-0046, Japan*
(Received 1 August 2005; published 20 October 2005)

The magneto-optical Kerr effect (MOKE) has been investigated for ferrimagnetic spinel compounds $M\mathrm{Cr}_2\mathrm{S}_4$ (M=Mn and Fe). In $\mathrm{FeCr}_2\mathrm{S}_4$, the gigantic magneto-optical response, reaching up to 4.3° in Kerr rotation, is observed at the energy of the intra-atomic *d-d* transition of Fe^{2+}, ${}^5E \rightarrow {}^5T_2$. By analyzing the resonance feature in the framework of the ligand field theory, we have clarified that the large oscillator strength enhanced by the strong covalency of the ligand sulfur as well as the local breakdown of inversion symmetry at the Fe^{2+} site is responsible for the gigantic signal. In $\mathrm{MnCr}_2\mathrm{S}_4$, the spin-*forbidden d-d* transition (${}^6A_1 \rightarrow {}^4T_1$) of Mn^{2+} is revealed in the MOKE spectra, which is not discernible in the optical reflectivity spectra.

DOI: 10.1103/PhysRevB.72.155114 PACS number(s): 78.20.Ls, 71.70.Ch, 71.70.Ej

I. INTRODUCTION

The magneto-optical Kerr effect (MOKE) in ferromagnets is the key subject of the current magneto-optical recording and the optical communication.[1,2] Its importance is still growing due to the great demand for more functional magneto-optical disks and optical isolators. One approach to the improvement of devices is a search for suitable materials, which show large MOKE signals under small magnetic field at high temperature. Such researches have been continuing in these several decades, developing the knowledge of how to enhance the MOKE responses. Besides resorting to the artificial superlattices,[3] we can choose either of at least two ways. One is a use of the so-called "plasma resonance," which is only possible in a metallic system.[4] The magneto-optical Kerr rotation θ and ellipticity η are connected with the dielectric tensor as

$$\theta + i\eta = \frac{\varepsilon_{xy}}{(1-\varepsilon_{xx})\sqrt{\varepsilon_{xx}}}. \quad (1)$$

Therefore, θ and η seemingly become large at the plasma energy, where $\mathrm{Re}(\varepsilon_{xx}) \sim 0$ is established. This mechanism is responsible for the enhanced MOKE in the rare-earth chalcogenides CeS, CeSe, CeSb, CeTe, TmS, TmSe, US, and $\mathrm{USb}_{0.8}\mathrm{Te}_{0.2}$, producing 2°–20° Kerr rotation and/or ellipticity.[5] However, it should be noted that these experiments are done in restricted temperature and/or magnetic field regions, typically 1–2 K and 4–10 T, because these materials are antiferromagnets with weak magnetic interactions. Another way to enhance the magneto-optical response is to make the MOKE resonant with an intra-atomic *d-d* transition. This strategy is important as it is applicable to insulating (transparent) magnets, which are necessary for optical isolators. After the Jung's pioneering work[6] on Cr^{3+} *d-d* transition, ${}^4A_2 \rightarrow {}^4T_1(t_2^2 e)$, in CrBr_3, Carnall *et al.* and Ahrenkiel *et al.* have found that $\mathrm{CoCr}_2\mathrm{S}_4$ with T_C of 230 K show the magneto-optical response as large as 4° at the energy of the Co^{2+} *d-d* transition.[7,8] This work has an important implication that a number of spinel compounds may have latent possibilities to show the gigantic MOKE response in the near-infrared region.

The aim of the present work is to expand the research by Carnall *et al.* and Ahrenkiel *et al.* to other related compounds $M\mathrm{Cr}_2\mathrm{S}_4$ (M=Mn,Fe), which also form the normal spinel structure. We performed the MOKE measurement over a wide photon-energy region of 0.2–4.5 eV and observed the 4.3° MOKE signal in $\mathrm{FeCr}_2\mathrm{S}_4$ and a spin-*forbidden d-d* transition in $\mathrm{MnCr}_2\mathrm{S}_4$. These observations are enabled by the absence of local inversion symmetry at the M site as well as the strong covalency effect.

$\mathrm{FeCr}_2\mathrm{S}_4$ is a ferrimagnetic insulator with T_C=170 K, where spins at tetrahedral Fe^{2+} and octahedral Cr^{3+} sites are antiparallel to each other.[9] This material shows large negative magnetoresistance near the Curie temperature.[10] The crystal symmetry remains cubic down to ~10 K, where the heat capacity shows a broad hump, as recently understood as the transition to the orbital-glass state.[11] The magnetic anisotropy constant reaches $K_1 \sim 3-6\times10^5$ N/m$^2 > 0$ at 5 K.[12] $\mathrm{MnCr}_2\mathrm{S}_4$ is ferrimagnetic below 65 K and it undergoes a first order phase transition toward the canted spin state at 5 K.[13]

II. EXPERIMENT

The single crystals of $M\mathrm{Cr}_2\mathrm{S}_4$ (M=Mn,Fe) were grown by a chemical vapor transport method with CrCl_3 as a transport agent.[14] We characterize the octahedral-shaped crystals by powder x-ray diffraction and inductively coupled plasma spectrometry, confirming that the obtained crystals are single phase with expected chemical formula. Magnetic properties measured with a superconducting quantum interference device magnetometer and electrical resistivities coincide well with the previous results. All optical measurements were carried out on the as-grown [111] surface, since it was noticed that the mechanical polishing procedure enlarges the coercive force, making the reverse of magnetization by a permanent magnet impossible. Reflectivity measurements were performed using a Fourier-transform interferometer for 0.1–0.8 eV and a grating monochromator for 0.6–32 eV.

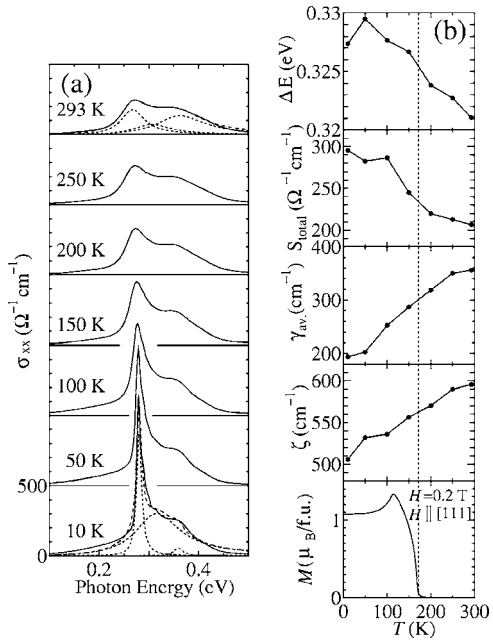

FIG. 1. (a) Optical conductivity spectra in the energy region of 0.1–0.5 eV for $FeCr_2S_4$. The broken lines represent the results of fitting with the three-component Lorentz oscillator model. (b) Temperature dependence of the crystal field splitting ΔE, the sum of oscillator strengths S_{total}, the average damping constant γ_{av}, the spin-orbit coupling constant ζ, and magnetization M.

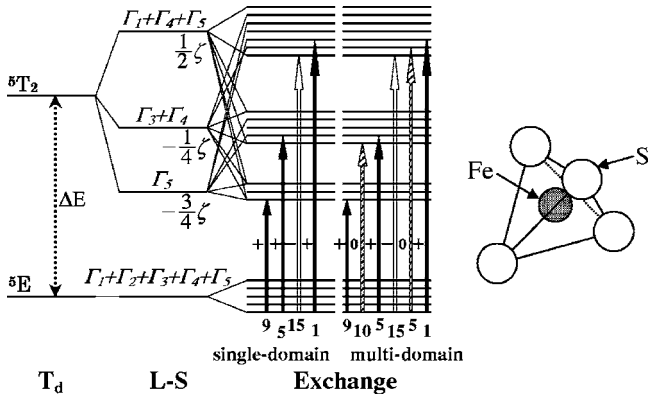

FIG. 2. The *d-d* transition of Fe^{2+} in the tetrahedral-coordination environment, $^5E \rightarrow {}^5T_2$, analyzed by the ligand field theory. The light **k** vector is set to [001] direction. In the "single domain" panel, all the spins are assumed to be aligned to the [001] direction, whereas in the "multidomain" panel, there are an equal number of [100], [010], and [001] magnetic domains. The ratios of the oscillator strength are shown for the $\Delta M_z = +1, 0, -1$ transition, which are represented by the filled, hatched, and open arrows, respectively.

Optical conductivity spectra $\sigma(\omega)$ were obtained from reflectivity spectra $R(\omega)$ by the Kramers-Kronig analysis. The MOKE measurements were done using a polarization modulation technique with a photoelastic modulator (PEM) in polar Kerr configuration.[15] The new aspect of our experiment is the measurement in the midinfrared region down to 0.2 eV, which is enabled by the combination of a polarization modulation technique (PEM: Hinds, Model II/S50) and Fourier-transform infrared spectroscopy. The magnetic field of 0.2 T was applied by a permanent magnet along the [111] direction. We note that the magnetization of the sample is in the multidomain state with [100], [010], and [001] directions due to the strong magnetic anisotropy.

III. RESULTS AND DISCUSSION

A. $FeCr_2S_4$

As shown in Fig. 1(a), optical conductivity spectra of $FeCr_2S_4$ has a sharp peak structure around 0.3 eV. This feature is also observed in $MgAl_2O_4$:Fe,[16] CdTe:Fe,[16] ZnS:Fe,[16,17] and $CdIn_2S_4$:Fe,[18] being ascribed to a spin-allowed intra-atomic *d-d* transition of Fe^{2+}, $^5E \rightarrow {}^5T_2$, in the tetrahedral-coordination environment. Since Fe^{2+} ions occupy two sites connected with inversion operation in the primitive unit cell, this transition is expected to show Davydov splitting[19] as ^5E_g, $^5E_u \rightarrow {}^5T_{2g}$, $^5T_{1u}$. One transition ($^5E_g \rightarrow {}^5T_{1u}$) is a parity-odd dipole-allowed transition since $^5E_g \times {}^5T_{1u} = {}^5T_{1u} + {}^5T_{2u}$, whereas another transition ($^5E_g \rightarrow {}^5T_{2g}$) is a parity-even one, being silent in the reflectivity measurement. Hereafter, to avoid confusion, we index the *d-d* transition by the local symmetry T_d, neglecting the effect of Davydov splitting.

As can be seen in Fig. 1(a), the *d-d* transitions at all temperatures exhibit fine structures. There might be at least three possible origins for it. One is the lower-symmetry ligand field at the Fe^{2+} site, however, it is known that the site symmetry remains cubic without any structural phase transition down to $T \sim 10$ K.[11] The second possibility is the exchange splitting, however, this is effective only below T_C. The third and the most plausible origin is the effect of spin-orbit coupling. We have carried out calculations on the effect of the spin-orbit coupling and the exchange splitting, based on the strong-coupling scheme of the ligand-field theory (Fig. 2).[20,21] The calculations were done in two situations, where the magnetic moments are aligned to the magnetic easy-axis [001] alone, or otherwise they are aligned along one of the equivalent $\langle 001 \rangle$ axes which are all easy axes (multidomain case). In both cases, the light **k** vector is assumed to be normalized to the (001) surface.[22] In the ideal case, we can analyze our experimental data within the above-mentioned multidomain case, however, it should be noted that the analysis including many parameters sometimes reduce the reliabilities of the obtained results. Therefore, neglecting the effect of exchange splitting, we adopt the three-component Lorentz model:

$$\sigma = \sum_j \frac{S_j \omega^2 \omega_j \gamma_j}{(\omega_j^2 - \omega^2 + \gamma_j^2)^2 + 4\omega^2 \gamma_j^2}, \tag{2}$$

where $\omega_1 = \Delta E - \frac{3}{4}\zeta$, $\omega_2 = \Delta E - \frac{1}{4}\zeta$, $\omega_3 = \Delta E + \frac{1}{2}\zeta$. Here, ΔE, ζ, S_j, γ_j, are the crystal-field splitting parameter, the spin-orbit coupling constant, the oscillator strength, and the damping constant for the jth transition, respectively. The fitted results are represented in Figs. 1(a) and 1(b), where $\gamma_{\text{av}} = (\gamma_1 + \gamma_2 + \gamma_3)/3$ and $S_{\text{total}} = S_1 + S_2 + S_3$.[23] ΔE at the ground state is

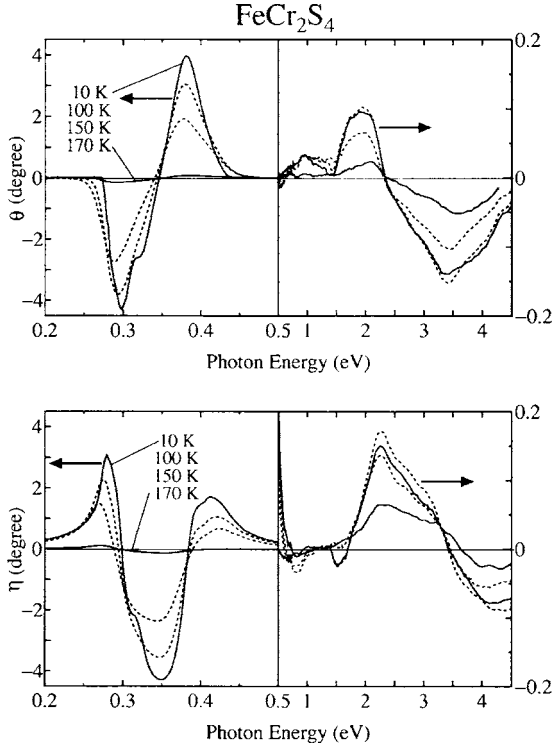

FIG. 3. Temperature dependence of the magneto-optical Kerr rotation (θ) and ellipticity (η) spectra of $FeCr_2S_4$ in the energy region of 0.2–4.5 eV. The abscissa scale is magnified for the *d-d* transition of Fe^{2+}, $^5E \rightarrow {}^5T_2$. Note that the ordinate scale is also different between 0.2–0.5 eV and 0.5–4.5 eV.

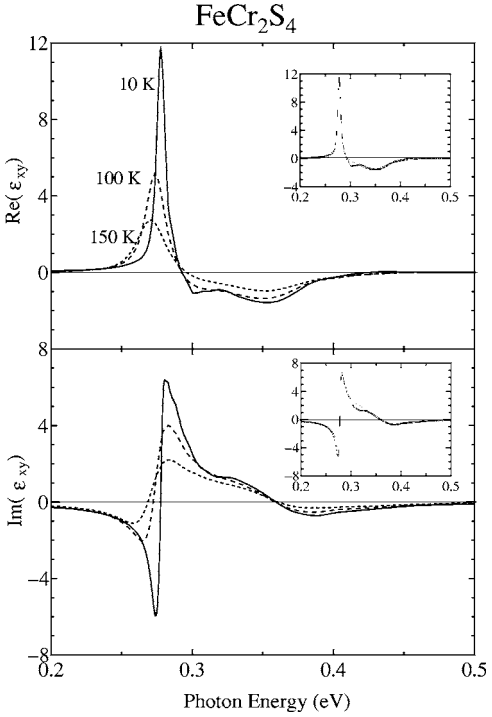

FIG. 4. Temperature dependence of the real and imaginary part of ε_{xy} for the *d-d* transition of Fe^{2+}, $^5E \rightarrow {}^5T_2$ in $FeCr_2S_4$. The results of fitting for the spectra at 10 K in the framework of the ligand field theory are shown in the insets.

relatively small, 0.321 eV, being consistent with the both facts that Fe^{2+} is coordinated by small number (4) of ligands and that the ligand is sulfur with strong covalent character. ζ at $T=10$ K reaches 596 cm^{-1}, which is even *larger* than that of free Fe^{2+} 410 cm^{-1} (Ref. 20). Although this value is unnatural in view of usual understanding of the covalency effect, the reason is not clear at present. All the optical parameters show systematic temperature dependence without any abrupt change at T_C. The increase of ΔE with decreasing temperature corresponds to the shrinkage of the lattice constants. The growing hybridization between Fe^{2+} *d* orbitals and S^{2-} *p* orbitals with decreasing temperature makes S_{total} larger and ζ smaller. With lowering temperature, γ_{av} becomes small, indicating the reduction of thermal broadening (coupling to lattice phonons).

Figure 3 represents the MOKE spectra of $FeCr_2S_4$ at various temperatures. Note the change in ordinate and abscissa scales at 0.5 eV. The spectral feature around 0.3 eV corresponds to the above-mentioned Fe^{2+} *d-d* transition and another around 3 eV originates from the S $3p \rightarrow$ Cr $3d$ charge transfer (CT) transition. The 4.3° MOKE signal at 10 K is the largest among that of known insulating magnets.

In Fig. 4, we depict the real and imaginary part of the off-diagonal component of the dielectric tensor in the energy region of Fe^{2+} *d-d* transition, which are deduced from Eq. (1).[24] The shape of spectrum is the so-called diamagnetic type, however, the high energy parts are broadened by the enhanced damping effect. As in the optical conductivity spectra, we have tried to fit the ε_{xy} spectra with the three-component Lorentz model:

$$\varepsilon_{xy} = \frac{2\pi}{i} \sum_j \omega_j \frac{S_j^+ - S_j^-}{\omega_j^2 - (\omega + i\gamma_j)^2}, \tag{3}$$

which is deduced from the microscopic calculation of ε_{xy} based on the Kubo-formula[25] with the approximation of $\omega \sim \omega_j$. Here, S_j^+ and S_j^- are the oscillator strength of the *j*th oscillator for right and left handed circular-polarized light, respectively. Although we set S_1, S_2, and S_3 as independent parameters in the analysis of optical conductivity spectra, we now put the restriction as $S_1^+=9S$, $S_1^-=0$, $S_2^+=5S$, $S_2^-=0$, $S_3^+=0$, $S_3^-=15S$. This is because the sum rule $\Sigma_j S_j^+ - S_j^- = 0$, deduced from the ligand field theory, should hold for the MOKE spectra of the *d-d* transition. The fitted results for $T=10$ K are shown in the inset of Fig. 4. The obtained parameters are $\Delta E=0.316$ eV and $\zeta=412$ cm^{-1}, being consistent with the values obtained from optical conductivity spectra.

It may be useful to explore how to maximize the MOKE signal in the framework of our analysis. By changing the parameters around the fitted values, we know that the following conditions are suitable for the further enhancement of MOKE signals: (1) small γ_j, (2) large ζ, and (3) large S_j^+ and S_j^-, being in agreement with our intuition. It is expected that $FeCr_2S_4$ actually fulfills, more or less, these conditions. In particular, we notice that the oscillator strength is greatly enhanced in $FeCr_2S_4$ owing to the two facts that *d-d* transition is dipole-allowed due to the absence of local inversion

symmetry at the Fe^{2+} site and that the effect of covalency is strong in the chalcogenide, compared with oxides and halides.

As for the temperature dependence of the MOKE spectra, the peak values of magneto-optical response around the Fe^{2+} *d-d* transition monotonically increases with decreasing temperature. This is in contrast to the temperature dependence of magnetization in $H=0.2$ T [Fig. 1(b)], which decreases below 120 K, indicating the evolution of magnetic anisotropy. This is because MOKE reflects the relevant electronic state of the system, not simply the total magnetization value.

B. $MnCr_2S_4$

We now proceed to the MOKE spectra of $MnCr_2S_4$. As shown in Fig. 5, there are discerned sharp structures around 1.8 eV in addition to the structure around 3 eV originating from S $3p \rightarrow$ Cr $3d$ CT excitation (inset in Fig. 5). Since the ligand field theory does not permit the appearance of any spin-allowed *d-d* transitions of Mn^{2+}, we have to pursue other possibilities. A hint is obtained by the reported magnetoreflectance spectra of $Zn_{0.72}Mn_{0.28}Te:Mn$,[26] where the similar absorptions are observed around $\omega \sim 2.2$ eV and ascribed to a spin-*forbidden d-d* transition, ${}^6A_1 \rightarrow {}^4T_1$. A similar interpretation may apply to the structures of the present spectra. The weak oscillator strength of this transition is ascribed to the spin-orbit coupling. The transition energy calculated by the strong-coupling scheme of the ligand field theory is $\omega = 10B + 6C - \Delta E$, where B and C are Racah parameters. If we take the free-ion value $C/B = 4.48$ (Ref. 20) as the ratio between B and C and neglect the effect of $\Delta E(\sim 0)$, we can estimate Racah parameters as $B \sim 372$ cm^{-1}. This is 43% of the free-ion value 860 cm^{-1} and should be realized as the consequence of the strong hybridization between Mn^{2+} d orbitals and S^{2-} p orbitals. As the temperature decreases, the spectra show distinct redshift. This may be caused by the temperature renormalized Racah parameters due to the enhanced covalency effect and/or by the enlarged ΔE. Incidentally, these weak transitions were not discernible in the ordinary optical reflectivity spectra. This confirms again the utility of the MOKE spectroscopy.

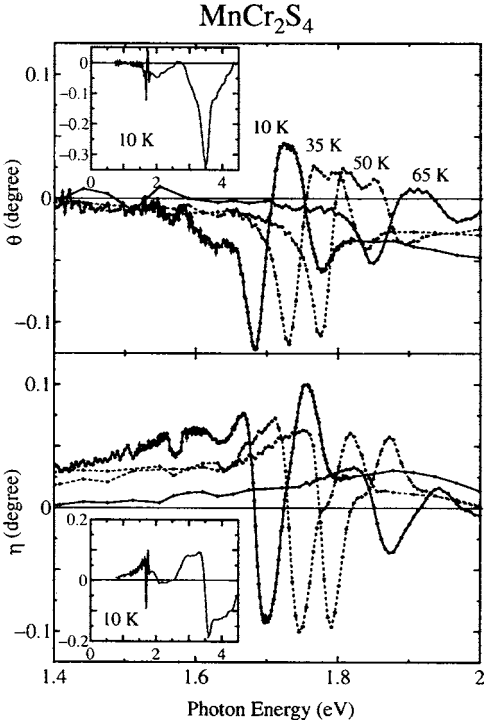

FIG. 5. Temperature dependence of the magneto-optical Kerr rotation (θ) and ellipticity (η) spectra for $MnCr_2S_4$. The main panel is that of the energy region of the *d-d* transition of Mn^{2+}, ${}^6A_1 \rightarrow {}^4T_1$. Insets show the spectra at $T=10$ K in an extended photon energy region of 0.7–4.5 eV.

IV. SUMMARY

To summarize, we have measured the MOKE spectra of MCr_2S_4 (M=Mn,Fe) in the wide energy region (0.2–4.5 eV). For $FeCr_2S_4$, the spectra show gigantic MOKE response (as large as 4.3°) resonant with the intraatomic *d-d* transition of Fe^{2+}. By the analysis based on the ligand field theory, we have clarified that the absence of local inversion symmetry at the Fe^{2+} site as well as the strong covalency effect in chalcogenide is essential for the gigantic MOKE. For $MnCr_2S_4$, we could unravel the spin-forbidden *d-d* transition of Mn^{2+} and deduce the Racah parameters.

[1] *Spin-Orbit-Influenced Spectroscopies of Magnetic Solids*, edited by H. Ebert and G. Schutz (Springer-Verlag, Berlin, 1996).
[2] *Magneto-Optics*, edited by S. Sugano and N. Kojima (Springer-Verlag, Berlin, 1999).
[3] T. Katayama, Y. Suzuki, H. Awano, Y. Nishihara, and N. Koshizuka, Phys. Rev. Lett. **60**, 1426 (1988).
[4] H. Feil and C. Haas, Phys. Rev. Lett. **58**, 65 (1987).
[5] W. Reim, O. E. Usser, J. Schoenes, E. Kaldis, P. Wachter, and K. Seiler, J. Appl. Phys. **55**, 2155 (1984); J. Schoenes and W. Reim, J. Magn. Magn. Mater. **54–57**, 1371 (1986); R. Pittini, J. Schoenes, and P. Wachter, Phys. Rev. B **55**, 7524 (1997); F. Salghetti-Drioli, K. Mattenberger, P. Wachter, and L. Degiorgi, Solid State Commun. **109**, 687 (1999).
[6] W. Jung, J. Appl. Phys. **36**, 2422 (1965).
[7] E. Carnall, D. Peterson, and T. J. Coburn, Mater. Res. Bull. **7**, 1361 (1972).
[8] R. K. Ahrenkiel, T. H. Lee, S. L. Lyu, and F. Moser, Solid State Commun. **12**, 1113 (1973); R. K. Ahrenkiel, T. J. Corburn, and E. Carnali, IEEE Trans. Magn. **10**, 2 (1974); R. K. Ahrenkiel, S. L. Lyu, and T. J. Coburn, J. Appl. Phys. **46**, 894 (1975).
[9] G. Shirane, D. E. Cox, and S. J. Pickart, J. Appl. Phys. **35**, 954 (1964).
[10] A. P. Ramirez, R. J. Cava, and J. Krajewski, Nature (London) **386**, 156 (1997).
[11] R. Fichtl, V. Tsurkan, P. Lunkenheimer, J. Hemberger, V. Fritsch, H.-A. Krug von Nidda, E.-W. Scheidt, and A. Loidl, Phys. Rev.

Lett. **94**, 027601 (2005).
[12] R. P. Stapele, J. S. van Wieringen, and P. F. Bongers, J. Phys. (Paris), Colloq. **32**, 53 (1971).
[13] V. Tsurkan, M. Mucksch, V. Fritsch, J. Hemberger, M. Klemm, S. Klimm, S. Korner, H.-A. Krug von Nidda, D. Samusi, E.-W. Scheidt, A. Loidl, S. Horn, and R. Tidecks, Phys. Rev. B **68**, 134434 (2003).
[14] H. V. Philipsborn, J. Cryst. Growth **9**, 296 (1971).
[15] K. Sato, J. Appl. Phys. **20**, 2403 (1981).
[16] G. A. Slack, F. S. Ham, and R. M. Chrenko, Phys. Rev. **152**, 376 (1966).
[17] F. S. Ham and G. A. Slack, Phys. Rev. B **4**, 777 (1971).
[18] S. Wittekoek, R. P. van Stapele, and A. W. J. Wijma, Phys. Rev. B **7**, 1667 (1973).
[19] A. S. Davydov, *Theory of Molecular Excitons* (Plenum Press, New York, 1971).
[20] S. Sugano, Y. Tanabe, and H. Kamimura, *Multiplets of Transition-Metal Ions in Crystals* (Academic, New York, 1970).
[21] J. S. Griffith, *The Theory of Transition-Metal Ions* (Cambridge University Press, Cambridge, 1961).
[22] Our experiments were in fact done on the (111) surface, however we expect no essential difference.
[23] The ratio of $S_1:S_2:S_3$ is deviated from 3:5:7, which is expected from the ligand field theory, suggesting that the degree of mixing of S^{2-} *p*-orbital with Fe^{2+} *d* orbital is energy dependent in this compound.
[24] The ε_{xx} spectra of the multidomain state with [100], [010], and [001] directions are expected to be the same as that obtained in the reflectivity measurement.
[25] C. S. Wang and J. Callaway, Phys. Rev. B **9**, 4897 (1974).
[26] Y. R. Lee, A. K. Ramdas, and R. L. Aggarwal, Phys. Rev. B **33**, 7383 (1986).